Fermi National Accelerator Laboratory

FERMILAB-Pub-81/14-THY
January, 1981

Beyond Upsilon: Heavier Quarkonia and the Interquark Force

PETER MOXHAY and JONATHAN L. ROSNER
School of Physics and Astronomy
University of Minnesota, Minneapolis, Minnesota 55455

and

C. QUIGG
Fermi National Accelerator Laboratory
P.O. Box 500, Batavia, Illinois 60510

(Received

ABSTRACT

A quarkonium potential constructed by inverse-scattering methods from the masses and leptonic decay widths of the upsilon vector mesons provides a basis for extrapolation to heavier quark-antiquark bound states. Level spacings and leptonic widths are predicted for systems with ground-state masses up to 60 GeV/c^2. It is found that present uncertainties in the potential at short distances would be most conclusively resolved by measurement of the 1^3S_1 leptonic decay rate. Less definitive but still of value would be determinations of the 2S-1S or 2S-2P level spacings, and measurement of the ratio of 2S and 1S leptonic

PACS numbers: 12.40.Qq, 14.40.Pe

widths. Other properties of the next quarkonium family are less sensitive indicators of short-range behavior, and can be anticipated with some confidence from experimental results already in hand. These serve to test further the flavor-independence of the interquark potential.

I. INTRODUCTION

Interest is high in families of heavy mesons beyond J/ψ and Υ both for what they would divulge about constituent spectroscopy and for the unique insight they could provide into the quark-antiquark interaction at short distances.[1] In this paper we use inverse scattering techniques[2] to explore the nature of the information that heavy quarkonium states can reveal about the strong interaction, and to refine our expectations for the properties of such systems.

In the preceding paper,[3] experimental information on quarkonium levels was used to construct interquark potentials. The agreement between potentials constructed independently using either charmonium states or upsilon states constitutes evidence that the force between quarks is flavor-independent at distances between 0.1 fm and 1 fm, where the potentials are well-determined. A natural extension of this work is the extrapolation to systems composed of heavier quarks. A similar extrapolation from the charmonium system successfully anticipated the properties of the upsilons.[4] As we shall see in greater detail below, projections to heavier masses involve the use of potentials not only where they are reliably determined, but also at shorter distances, where the form of the potential is considerably less certain.

To illustrate, let us summarize briefly what was learned from the J/ψ family about the upsilons. It was found that any potential which reproduced (by construction) the masses and leptonic widths of $\psi(3097)$ and $\psi(3686)$ and which gave correctly the spin-averaged mass of the 2^3P_J levels, $\langle M(\chi)\rangle = 3.52$ GeV/c^2, would lead to approximately the observed T-T' spacing. The leptonic decay width of T' was also predicted with sufficient precision to allow an early determination[5] of the b-quark charge as $e_b=-1/3$. In contrast, the potentials constructed from charmonium allowed considerable latitude in predictions for the leptonic width of the T ground state. Of the observables we shall consider, the 1S leptonic width has the greatest sensitivity to the short-range part of the potential.[6]

Extrapolating from ψ to T involved a three-fold increase in the quark-mass scale. Although the mass (not to mention the existence) of the next quarkonium system is in doubt, no less a factor seems required for extrapolation from the b-quark to the sixth quark.[7] However, given the shape of the interquark potential determined by inverse scattering methods, we believe that it is prudent to extrapolate no more than sixfold in the quark mass. Our caution is motivated by experience with known potentials. From the 10 GeV/c^2 upsilon family, we therefore limit our considerations to ($Q\bar{Q}$) systems below 60 GeV/c^2.

While our chief interest here is the pursuit of the inverse scattering program, this exercise also illuminates comparisons of new data with predictions of explicit potential models. It helps distinguish predictions dictated by previous data from those that are explicitly consequences of hitherto untested theoretical hypotheses.

We begin by reviewing in Sec. II some useful observables and their significance for the determination of potentials. Elementary scaling arguments[8,9] are used to illustrate the probable range of these parameters. In Sec. III, we choose a representative set of potentials constructed from upsilon data, with the aid of a minimal set of constraints from charmonium. Details were presented in the preceding paper,[3] so we can be very brief. Results for systems composed of heavier quarks are presented in Sec. IV. These are compared with the consequences of a representative explicit potential.[10] This permits an assessment of how restrictive such a theoretically-inspired potential is, in comparison to the model-independent and theoretically unbiased inverse scattering approach. Our conclusions are summarized in Sec. V, where we recapitulate the predictions which are most stable and those which are most sensitive to the *terra incognita* of short distances. An Appendix addresses technical matters regarding the reliability of the inverse scattering method for extrapolation to higher masses in potentials which are singular at the origin.

II. OBSERVABLES

Many properties of quarkonium levels give immediate information about the form of the interquark force in a particular distance regime.[9] We recall here some of the ways in which the potential can be characterized by quarkonium observables.

A. 2S-1S Level Spacing

Comparison of the charmonium and upsilon levels led to the conclusion that if the interquark potential could be represented as a power-law,

$$V(r) = \lambda\ r^{\nu}, \tag{1}$$

over the region probed by ψ, ψ', Υ, and Υ', then the effective power ν was close to zero.[8,9,11-13] (The nontrivial potential corresponding to $\nu=0$ is $V(r)=C\ \ln(r)$.) This conclusion follows from the scaling behavior

$$\Delta E \propto m_Q^{-\nu/(2+\nu)} \tag{2}$$

appropriate for a fixed potential, and the observed near-equality of ψ and Υ level spacings,

$$M(\psi')-M(\psi) \approx M(\Upsilon')-M(\Upsilon). \tag{3}$$

In any potential with a short-range Coulomb-like singularity (which may be anticipated on the basis of one-gluon exchange), heavier quarks will probe the singularity more deeply, the effective power ν will decrease below zero, and the 2S-1S level spacing will increase from its value in the upsilon family,[14]

$$M(\Upsilon')-M(\Upsilon) = 0.56\pm0.01\ \text{GeV}/c^2. \qquad (4)$$

B. 2S-2P Splitting

The splitting between[15] the 2S and 2P levels (which are degenerate in the Coulomb problem) gives another measure of the shape of the potential. The ratio

$$R_{SP} \equiv \frac{M(2S)-M(2P)}{M(2S)-M(1S)}, \qquad (5)$$

which is independent of the potential strength λ, is a convenient parameter. Its behavior as a function of the effective power ν is given in Fig. 13 of Ref. 9; representative values are $R_{SP}=(0.5,0.255,0)$ for $\nu=(2,0,-1)$. Experimentally, $R_{SP}=0.28$ for charmonium, consistent with our earlier inference that the effective power is near zero. If $\nu\simeq0$ also characterizes the upsilon spectrum, we would expect the center-of-gravity of the 2^3P_J states to lie at

$$\langle M(\chi_b)\rangle \simeq M(\Upsilon')-140\ \text{MeV}/c^2. \qquad (6)$$

Any smaller 2S-2P spacing would be suggestive of more singular behavior of the potential at short distances. For still heavier quarks, the presence of a Coulomb-like singularity would manifest itself in a value of R_{SP} rather less than 0.255.

C. Leptonic Decay Widths

The square of the wavefunction of an n^3S_1 bound state at zero quark-antiquark separation is related to the mass and leptonic width of the state by[16]

$$|\Psi_n(0)|^2 = (3/16\pi N_c \alpha^2 e_Q^2)\cdot\rho\cdot M_n^2\, \Gamma(V_n \to e^+e^-), \qquad (7)$$

where N_c is the number of colors of the bound quark and e_Q is its charge, $\alpha \simeq 1/137$ is the fine-structure constant, and M_n is the mass of the vector state V_n. The multiplicative factor ρ is equal to unity in the nonrelativistic limit. The quantity $|\Psi_n(0)|^2$ has simple dependences upon the quark mass and the principal quantum number in power-law potentials.[8,9] If the variation of ρ with principal quantum number is neglected within a specific quarkonium family, the ratio

$$R_{21} \equiv \frac{M^2(2S)\Gamma_{ee}(2S)}{M^2(1S)\Gamma_{ee}(1S)} \qquad (8)$$

will be equal to

$$R_{21} = |\Psi_2(0)|^2/|\Psi_1(0)|^2, \tag{9}$$

for which the dependence upon the effective power ν is plotted in Fig. 15 of Ref. 9. Representative values are R_{21}=(1, 0.51, 1/8) for ν=(1,0,-1), independent of the potential strength λ. Experimental values are

$$R_{21} = \begin{cases} 0.62 \pm 0.17 & (\psi), \\ 0.51 \pm 0.08 & (\Upsilon), \end{cases} \tag{10}$$

consistent with each other and with $\nu \simeq 0$.

The magnitude of the 1S leptonic width is also indicative of the short-range character of the potential. The quantity $\Gamma_{ee}(1S)/e_Q^2$ is known to be approximately universal (see Fig. 17 of ref. 9) for the vector mesons ρ^0,ω,ϕ,ψ, and Υ or equivalently for the u,d,s,c, and b quarks. Neglecting what might be expected to be a significant variation of the parameter ρ from the lightest family to the heaviest, one would infer from eq. (7) that

$$|\Psi(0)|^2 \propto M_V^2. \tag{11}$$

If in addition we neglect binding energies compared to quark masses (an unwarranted assumption for ρ^0,ω,ϕ,ψ) so that $M_V \propto m_Q$, then elementary scaling arguments[8,9] which imply that

$$|\Psi(0)|^2 \propto m_Q^{3/(2+\nu)} \tag{12}$$

lead us to conclude that the effective power is $\nu \simeq -1/2$. Both of the questionable approximations in this line of argument should be more trustworthy in the comparison of the upsilons and the next heavier family.

Leptonic widths of the higher s-waves are less sensitive to new short-range physics, and are more stably determined by the physics of ψ and Υ. Thus they are well-suited for measuring new-quark charges.[5]

D. Flavor Threshold

The threshold for pair production of mesons bearing the flavor carried by a heavy quark Q will be marked by a rise in the quantity

$$R \equiv \frac{\sigma(e^+e^- \to \text{hadrons})}{\sigma(e^+e^- \to \mu^+\mu^-)} \ . \tag{13}$$

This threshold energy, $E_{th}(Q\bar{Q})$, can be related very simply to the threshold energy $E_{th}(b\bar{b})$ for production of b-flavored particles, as[17]

$$E_{th}(Q\bar{Q}) \simeq E_{th}(b\bar{b}) + 2(m_Q - m_b) . \tag{14}$$

In the preceding paper,[3] the flavor threshold in the upsilon system was estimated as

$$10.46\ \text{GeV} \leq E_{th}(b\bar{b}) \leq M(\Upsilon''') = 10.545\ \text{GeV}. \quad (15)$$

This implies that the flavor threshold for the next quarkonium family will lie at

$$E_{th}(Q\bar{Q}) \simeq 10.5\ \text{GeV} + 2(m_Q - m_b). \quad (16)$$

The relation (14) implies that flavor threshold occurs at a fixed "dissociation radius" for all heavy-quark systems, which is to say at a fixed position in the potential. The interval between the ground state 1^3S_1 level and flavor threshold therefore is directly related to the shape of the potential, and in particular to the depth of the well. In a potential $V = C \cdot \ln(r/r_0)$, which with $C = 0.7$ GeV approximately reproduces the properties of the upsilon states, one expects

$$E_{th}(Q\bar{Q}) - M(1S{:}Q\bar{Q}) = E_{th}(b\bar{b}) - M(\Upsilon) + \frac{C}{2}\ln(m_Q/m_b)$$
$$= (1.07 + 0.35\ \ln(m_Q/m_b))\ \text{GeV}. \quad (17)$$

For more singular potentials, corresponding to effective powers $\nu < 0$, the 1S bound states of heavy quarks will lie still deeper in the well, and the flavor threshold-1S interval will exceed the estimate (17).

E. Electric Dipole Transition Rates

We shall not calculate the E1 transition rates explicitly, because they depend cubically (thus sensitively!) on as-yet-unknown photon energies. Let us note, however, that they can provide useful information on the spatial sizes of quarkonium states, which do have simple scaling properties in power-law potentials.[8,9] Some specific examples have been given elsewhere[18,3] for charmonium and the upsilons.

III. POTENTIALS CONSTRUCTED FROM THE UPSILONS

The inverse-scattering methods that have been developed for the quarkonium problem[2] have been recapitulated in the preceding article.[3] The Υ(1S)-Υ(4S) levels have been shown to permit the reconstruction of the interquark potential with a degree of confidence in the interval 0.1 fm - 1 fm. In this region, the shape of the potential depends little on the assumed value of the b-quark mass, m_b. The other parameter of reflectionless approximants to confining potentials, the energy at which the continuous spectrum of the approximant begins, has been chosen as E_0=10.6 GeV, slightly above the position of Υ(4S).

Once E_0 and m_b have been selected, the potential is completely specified by the masses and wavefunctions squared at the origin of the four $^3S_1$ levels of the upsilon family.

According to eq. (7), the square of the wavefunction at the origin is known, up to a factor ρ, in terms of the mass and leptonic decay width of the vector meson. This factor has not been calculated from first principles for quarkonium. In the nonrelativistic limit ρ is equal to unity, but in the presence of strong interactions it is expected to exceed one. We have taken[3] the values $\rho=1, 1.4, 2$ as representative of the plausible range of values.

Although the choice of m_b has little effect on upsilon physics, it does influence slightly the shape of the potential, especially at short distances. To specify the mass of the b-quark we may appeal to the charmonium system, at the price of assuming the flavor-independence of the potential expected in theory and demonstrated in the preceding paper.[3] Observables in the charmonium system have a considerably greater sensitivity to the assumed value of the charmed-quark mass. The difference m_b-m_c is constrained in potential models to lie within rather narrow limits,[19] which we have argued in ref. 3 are given by

$$3.32\ \mathrm{GeV}/c^2 \le m_b-m_c \le 3.41\ \mathrm{GeV}/c^2. \qquad (18)$$

Thus, a variation in m_b from 4.5 to 5 GeV/c^2 induces a shift in m_c from about 1.1 to 1.6 GeV/c^2. This has a marked effect upon the ψ and ψ' leptonic widths, which vary approximately as $m_c^{3/2}$ for potentials characterized by $\nu_{eff}\approx 0$. Guided by the charmonium leptonic widths, we have taken the values

m_b=4.5, 4.75, and 5 GeV/c^2 corresponding to ρ=1, 1.4, and 2 (see Table III of Ref. 3). Slightly higher values of the b-quark mass (by perhaps 0.1 GeV/c^2) would also be satisfactory.

IV. EXTRAPOLATIONS IN THE HEAVY-QUARK MASS

Extrapolations based upon the three upsilon potentials constructed in the previous paper[3] are summarized in Figs. 1-3. For comparison, the consequences for heavy-quark systems of representative QCD-inspired explicit potentials[10] are also shown there.

We first draw attention to quantities which are relatively indifferent to the variations from potential to potential. The level schemes of Fig. 1 show that the 2S-3S interval, the 3S-4S interval, and the position of the 2S level with respect to flavor threshold each are predicted similarly in all six potentials. For any quark mass in the interval considered, the threshold-2S interval differs from potential to potential by no more than 80 MeV. These exemplify the class of predictions that depend on physics already known from charmonium and the upsilons, and do not test the short-distance part of the interaction. Important departures from these predictions would call into question the flavor-independence of the interaction or, within the framework of QCD, the assumption that the heavy quark is a color triplet.

More variation occurs in the predictions for the 2S-1S level spacing shown in Fig. 1 (and therefore in the threshold-1S interval), the ratio $R_{SP}=(M(2S)-M(2P))/(M(2S)-M(1S))$ plotted in Fig. 2, and the ratio of leptonic widths of the 2S and 1S levels depicted in Fig. 3. A rough correspondence may be noted between the consequences of the $\rho=1$, $m_b=4.5$ GeV/c^2 potential (designated by (a) in the figures) and the Buchmüller-Tye potential for $\Lambda_{\overline{MS}}=0.2$ GeV (e); and of the $\rho=1.4$, $m_b=4.75$ GeV/c^2 potential (b), the Richardson potential (d), and the Buchmüller-Tye potential for $\Lambda_{\overline{MS}}=0.5$ GeV (f). For this range of heavy-quark masses, the predictions of the $\rho=2$, $m_b=5$ GeV/c^2 potential (c) are those of potentials more singular near the origin than any of the potentials of Ref. 10. Note, however, that while the behavior of R_{SP} is monotonic for the (smooth and bottomless) explicit potentials, it is not for the potentials constructed using inverse-scattering techniques. For all of these observables, the predictions of the $\rho=2$, $m_b=5$ GeV/c^2 potential (c) lie outside the range delimited by the explicit potentials.

Among the observables we consider, the 1S leptonic width alone can provide a sensitive probe of the potential at short distances. Thus, for inverse scattering constructions the 1S leptonic width predicted by the deepest potential (c) is greater by a factor of about two than that implied by the shallowest potential (a).[20] Similarly for the explicit potentials, $\Gamma_{ee}(1S)$ is controlled by the strength of the Coulomb-like singularity, which is weakest for (e) the Buchmüller-Tye potential with $\Lambda_{\overline{MS}}=0.2$ GeV. For potentials which other observables have led us to place in correspondence, the inverse scattering method consistently leads to still smaller 1S leptonic widths than the explicit potentials do. There are two reasons for this difference. First, the potentials constructed from the upsilon are, by the nature of the inverse-scattering method, finite at the origin, whereas all the explicit potentials considered here are singular. A nonsingular power-law potential of the sort advocated by Martin,[13] which otherwise yields observables similar to those of potentials (a) and (e), leads to still smaller 1S leptonic widths than the potentials discussed here. Second, we have computed leptonic widths for the upsilon potentials assuming that the factor ρ of eq. (7) relating $|\Psi(0)|^2$ to the leptonic width is independent of the heavy-quark mass, whereas Buchmüller and Tye have adopted the form[21]

$$\rho = \left[1 - \frac{16\alpha_s}{3\pi} + \mathcal{O}(\beta^2)\right]^{-1} \tag{19}$$

analogous to radiative corrections in positronium. In eq. (19), α_s is the running coupling constant of the strong interactions and β is the velocity of the bound quark. This form and the evolution of α_s suggest that ρ should decrease toward unity as the quark mass increases. Through eq. (7), this behavior implies a gradual augmentation of the predicted leptonic widths, as the quark mass increases.

For quark masses exceeding about 12 GeV/c^2, which is to say greater than approximately 2-1/2 times the b-quark mass, the inverse-scattering potentials display an aberrant pattern of leptonic widths: the predictions do not decrease monotonically with increasing principal quantum number n. We regard this deportment as an artifact of the local oscillations in the reconstructed potentials. Similar characteristics were observed earlier[4] in analogous predictions for the upsilons, on the basis of potentials constructed from charmonium. The data (ref. 14) exhibit the conventional pattern, $\Gamma_{ee}(1S)>\Gamma_{ee}(2S)>\Gamma_{ee}(3S)>\Gamma_{ee}(4S)$. The explicit potentials manifest no unusual symptoms.

In Fig. 4 we depict the relative positions of the Υ and (QQ) levels for m_Q=20 and 30 GeV/c^2 in the ρ=1.4, m_b=4.75 GeV/c^2 potential, which was denoted (b) in previous figures. Flavor threshold for the $b\bar{b}$ system, estimated in ref. 3 to lie between 10.46 GeV/c^2 and Υ(4S;10.545), is indicated by the shaded band. Extending it to the right-hand side of the figures, as prescribed by eq. (14), we are led to expect seven narrow $^3S_1$ $(Q\bar{Q})$ levels if m_Q=20 GeV/c^2, and eight or nine if m_Q=30 GeV/c^2. These are in accord with model-independent expectations.[28]

Within the inverse-scattering formalism, it is a technical convenience to represent the input information on s-wave wavefunction normalization in terms of energy eigenvalues of even-parity bound states in a symmetric, one-dimensional potential.[23] By displaying the positions of these levels, which are unphysical from the point of view of the three-dimensional central potential problem, we gain a further appreciation of the distance scales that are important for determining the potential. The fictitious upsilon levels are indicated by dotted lines in Fig. 4. The position of the lowest-lying even-parity level is quite sensitive to the value of the parameter ρ, and to the absolute scale of the $\Upsilon(1S)$ leptonic width. It serves as a crude index of how large an extrapolation in quark mass is likely to be trustworthy. To extrapolate to a quark mass for which the 1^3S_1 level lies deeper in the potential than the lowest even-parity level used in the reconstruction would be rash. We refrain from doing so: the closest approach among the examples we present is for the case $\rho=1$, $m_b=4.5$ GeV/c^2, $m_Q=30$ GeV/c^2, for which the 1^3S_1 $(Q\bar{Q})$ level lies 230 MeV/c^2 above the lowest even-parity $(b\bar{b})$ level.

V. CONCLUSIONS

Inverse scattering techniques have been used to extrapolate from the observed attributes of the upsilon family to heavier quarkonium systems. Results of this program have been presented for $(Q\bar{Q})$ states with masses up to 60 GeV/c^2, and compared with expectations derived from specific potentials.

One category of predictions is common to all reasonably smooth potentials that describe the upsilons. For example, the 2S-3S and 3S-4S intervals are essentially determined by known physics. Any experimental departure from these predictions would indicate that the new systems are not composed of ordinary quarks, or that the strong interaction is not flavor-blind.

A second class of predictions primarily depends, within the context of the inverse scattering method, on the connection between the leptonic decay width and the square of the wavefunction at the origin. More generally, these observables are sensitive to the absolute scale of the leptonic widths of the upsilons. Quantities of interest include the 2S-1S level spacing, the ratio (M(2S)-M(2P))/(M(2S)-M(1S)), the ratio of 2S to 1S leptonic widths, and the distance between flavor threshold and the 1S level. Measurement of any of these quantities in heavier quarkonium systems would shed light on the quark-antiquark interaction at somewhat shorter distances than probed by charmonium and the upsilons.

Finally, the magnitude of the 1S leptonic width of heavy quarkonium emerges as the quantity uniquely sensitive to the structure of the strong interaction at short distances. That this should be so is particularly clear within the methodology of inverse scattering, as we have seen in § IV. The 1S leptonic decay rate can thus distinguish among potentials which agree in the interval now explored experimentally (0.1 fm - 1 fm), but differ at smaller quark-antiquark separations.

The inverse scattering approach has the virtue of relying in very direct fashion upon experimental data, and delimiting the region of space in which the potential is established. It clarifies the issue of what predictions follow from existing observations, and what predictions rely upon theoretical assumptions not yet implied by experiment. Many extrapolations based upon reconstructed potentials depend smoothly and systematically upon the quark mass. For other observables limitations and idiosyncrasies of the method become apparent. Artifacts of this technique are of two sorts: oscillations and finite depth-of-well. The inverse scattering algorithm leads unavoidably to potentials finite at zero quark-antiquark separation, and does not guarantee that potentials will increase monotonically with the separation. Ratios of leptonic widths are sensitive to local oscillations in the potential, while the magnitude of the 1S leptonic width is influenced by the finiteness of the reconstructed potential at the origin. Explicit potentials and elementary scaling laws both can avoid the oscillations. Explicit potentials also make definite predictions for the very short distance behavior. Of course, they need not be correct.

The present exercise has two aims. One is to identify a set of stable predictions which may serve as guides for experiment and for testing whether a new family of quarks obeys familiar dynamics. The other is to focus attention on observables which can only be predicted within wide limits. These will provide new information about the quark-antiquark interaction and significant tests of theoretically-inspired potentials. We thus regard the inverse-scattering method as a means for determining the interaction from quarkonium data, and as a tool for determining the extent to which predictions of specific potentials are explicitly dependent upon the underlying theoretical assumptions.

ACKNOWLEDGMENTS

Part of this research was carried out during visits by J.L.R. to Cornell University and Fermilab. He wishes to thank K. Gottfried, D. Yennie, and C. Quigg for extending the generous hospitality of these institutions. Work at the University of Minnesota was supported in part by the United States Department of Energy under Contract No. EY-76-C-02-1764. Fermilab is operated by Universities Research Association, under contract with the Department of Energy.

Discussions with K. Adams, O. Alvarez, J.D. Bjorken, W. Buchmüller, D. Creamer, E. Eichten, K. Gottfried, S. Herb, G.P. Lepage, M. Peskin, T.-M. Yan, and others at Cornell, Fermilab, and Minnesota are gratefully acknowledged. It is a pleasure to recognize the contributions of H.B. Thacker and J.F. Schonfeld to earlier phases of this program.

APPENDIX. QUALITY OF EXTRAPOLATIONS IN CONSTITUENT MASS FOR REFLECTIONLESS APPROXIMATIONS TO SINGULAR POTENTIALS

If the interquark potential is indeed singular at the origin, it is expected to be more singular than

$$V(r) = \ln(r/r_0) \tag{A.1}$$

and less singular than

$$V(r) = -1/r. \tag{A.2}$$

It is therefore of interest to test the reliability of the inverse-scattering method for mass extrapolations in these two potentials. The quality of the extrapolation in quarkonium is likely to be intermediate between the results found for these two cases.

Following the procedure we have used for quarkonium,[3] we approximate the Coulomb and logarithmic potentials by (symmetric) reflectionless potentials constructed from the four lowest-lying s-wave levels. With the parameter E_0 chosen by interpolation as

$$E_0 = \frac{3E(4S)+E(5S)}{4}, \tag{A.3}$$

and the constituent mass $m \equiv 1$, the parameters κ_i of the reflectionless approximant are determined as usual from the positions and wavefunctions at the origin of the input levels. The input data and derived parameters are collected in Table I.

We next solve the Schrödinger equation in the reconstructed potentials for various values of constituent mass m' exceeding the mass m for which the potentials were constructed. Results are shown in Figs. 5 and 6 as functions of m'/m. Extrapolations in the reconstructed logarithmic potential are faithful over a wider range than those in the Coulomb potential. Over the range $1 \le m'/m \le 6$, the 2S-1S spacing is reproduced within 3% for the logarithmic potential, but only within 20% for the Coulomb potential. Similarly, the quality of the computed ratio $R_{SP}=(E(2S)-E(2P))/(E(2S)-E(1S))$ deteriorates rapidly when $m'/m>4$ for the Coulomb potential, but remains accurate for the logarithmic potential. The ratio $|\Psi_2(0)|^2/|\Psi_1(0)|^2$ is reproduced within 25% in the logarithmic potential, but only within 50% in the Coulomb potential throughout the interval studied. Finally, the 1S wavefunction normalization $|\Psi_1(0)|^2$ is given within 5% of its true value for the logarithmic potential, for $m'/m<6$, but is quite unreliably predicted in the reconstructed Coulomb potential throughout the entire interval.

The decision to limit our quarkonium predictions to $m_Q/m_b<6$ is clearly a subjective one. Even within this range certain quantities can be predicted with more confidence than others.

Table I. Parameters entering reflectionless approximations to Coulomb and logarithmic potentials.

	$V(r)=\ln(r/r_0)$		$V(r)=-1/r$	
n	E(nS)	$\|\Psi_n(0)\|^2$	E(nS)	$\|\Psi_n(0)\|^2$
1	1.0443	0.0549	-0.25	0.039789
2	1.8474	0.0280	-0.0625	0.004974
3	2.2897	0.0191	-0.02778	0.001474
4	2.5957	0.0146	-0.01563	0.000622
5	2.8299		-0.01	
	$E_0=2.6543$		$E_0=-0.01422$	
i	κ_i		κ_i	
1	1.7199		1.3572	
2	1.2689		0.4856	
3	1.0829		0.3232	
4	0.8983		0.2197	
5	0.7631		0.1654	
6	0.6038		0.1164	
7	0.4666		0.0840	
8	0.2421		0.0375	

FOOTNOTES AND REFERENCES

1. T. Appelquist and H.D. Politzer, Phys. Rev. Lett. 34, 43 (1975).

2. H.B. Thacker, C. Quigg, and J.L. Rosner, Phys. Rev. D18, 274 (1978); ibid., D18 287 (1978); H. Grosse and A. Martin, Nucl. Phys. B148, 413 (1979); J.F. Schonfeld, et al., Ann. Phys. (N.Y.) 128, 1 (1980); I. Sabba Stefanescu, Karlsruhe report no. TKP 80-20 (unpublished).

3. C. Quigg and J.L. Rosner, Fermilab-Pub-81/13-THY (preceding paper).

4. H.B. Thacker, C. Quigg, and J.L. Rosner, Phys. Rev. D18, 287 (1978).

5. J.L. Rosner, C. Quigg, and H.B. Thacker, Phys. Lett. 74B, 350 (1978).

6. Hyperfine structure, which may also be an indicator of short-distance behavior, depends critically upon the Lorentz structure of the potential, about which model-independent methods have up to now been mute.

7. Studies of electron-positron anihilations at PETRA rule out a new charge-2/3 quark with mass less than about 18 GeV/c^2. A new quark of charge (-1/3) is also unlikely at masses below 15 GeV/c^2. See Ch. Berger, et al. (PLUTO Collaboration), Phys. Lett. 81B, 410 (1979); ibid., 91B, 148 (1980); R. Brandelik, et al. (TASSO Collaboration), ibid., 83B, 261 (1979); ibid., 86B, 243 (1979); ibid., 88B, 199 (1979); ibid., 89B, 418 (1980); Z. Phys. C4, 87 (1980); W. Bartel, et al. (JADE Collaboration), Phys. Lett. 88B, 171 (1979); ibid., 89B, 136 (1979); ibid., 91B, 152 (1980); D.P. Barber, et al. (Mark-J Collaboration), Phys. Rev. Lett. 44, 1722 (1980).

8. C. Quigg and J.L. Rosner, Comments Nucl. Part. Phys. 8, 11 (1978).

9. C. Quigg and J.L. Rosner, Phys. Rep. 56C, 167 (1979).

10. J.L. Richardson, Phys. Lett. 82B, 272 (1979); W. Buchmüller and S.-H. H. Tye, Fermilab-Pub-80/94-THY, unpublished.

11. C. Quigg and J.L. Rosner, Phys. Lett 71B, 153 (1977).

12. C. Quigg, in Proceedings of the 1979 International Symposium on Lepton and Photon Interactions at High Energies, edited by T.B.W. Kirk and H.D.I. Abarbanel (Fermilab, Batavia, Illinois, 1980), p. 239; J.L.Rosner, in Particles and Fields-1979, edited by B. Margolis and D.G. Stairs (American Institute of Physics, New York, 1980), p. 325; J.L. Rosner, "Quark Models," Lectures given at the NATO Advanced Study Institute, "Techniques and Concepts of High-Energy Physics," held at St. Croix, U.S. Virgin Islands, July 2-13, 1980 (to be published).

13. A. Martin, Phys. Lett. 93B, 338 (1980); CERN report No. TH.2980 (1980, unpublished).

14. S.W. Herb, et al., Phys. Rev. Lett. 39, 252 (1977), W.R. Innes, et al., ibid., 39, 1240 (1977); ibid., 39, 1640E(1977); K. Ueno, et al., ibid., 42, 486 (1979); Ch. Berger, et al. Phys. Lett. 76B, 243 (1978); Z. Phys. C1, 343 (1979); C.W. Darden, et al., Phys. Lett. 76B, 246 (1978); ibid., 80B, 419 (1979); J. Bienlein, et al., ibid., 78B, 360 (1978); D. Andrews, et al., Phys. Rev. Lett. 44, 1108 (1980); ibid., 45, 219 (1980); T. Böhringer, et al., 44, 1111 (1980); ibid., 45, 222 (1980); G.C. Moneti, et al., Syracuse report no. HEPSY 15-80 (1980, unpublished); C. Bebek, et al., Phys. Rev. Lett. 46, 84 (1981); B. Niczyporuk, et al., ibid., 46, 92 (1981). An up-to-date summary is given by K. Berkelman, "New Flavor

Spectroscopy," Cornell report No. CLNS 80/470 (unpublished).

15. Levels are labelled by the principal quantum number n, which is related to the radial quantum number n_r and the orbital angular momentum ℓ by $n=n_r+\ell$.

16. With $\rho=1$, this connection (up to the color factor) is due to R. Van Royen and V.F. Weisskopf, Nuovo Cim. 50, 617 (1967); ibid., 51, 583 (1967).

17. E. Eichten and K. Gottfried, Phys. Lett. 66B, 286 (1977); C. Quigg and J.L. Rosner, ibid., 72B, 462 (1978).

18. E. Eichten, et al.; Phys. Rev. D21, 203 (1980).

19. R.A. Bertlmann and A. Martin, Nucl. Phys. B168, 111 (1980); A.K. Common, University of Kent preprint (1980, unpublished).

20. The shapes of the upsilon potentials are compared in Fig. 5 of ref. 3, where the $\Lambda_{\overline{MS}}=0.5$ GeV potential of Buchmüller and Tye, ref. 10, is also shown.

21. The QED formula is due to R. Karplus and A. Klein, Phys. Rev. 87, 848 (1952). Multiplicative corrections to the orthoquarkonium decay rate have been investigated by many authors, including R. Barbieri, et al., Phys. Lett. 57B, 455 (1975), Nucl. Phys. B105, 125 (1976); W. Celmaster, Phys. Rev. D19, 1517 (1979); E. Poggio and H.J. Schnitzer, ibid., D20, 1175 (1979); ibid., D21, 2034 (1980); L. Bergström, H. Snellmann, and G. Tengstrand, Phys. Lett. 80B, 242 (1979); ibid., 82B, 419 (1979); Z. Phys. C4, 215 (1980); C. Michael and F.P. Payne, Phys. Lett. 91B, 441 (1980); B. Durand and L. Durand, Wisconsin preprint No. DOE/ER/00881-176 (1980, unpublished).

22. Quigg and Rosner, ref. 17.

23. The even-parity energy eigenvalues are given by the zeroes of the function defined in eq. (14) of ref. 3.

FIGURE CAPTIONS

Fig. 1: Level spacings for heavy quarkonia in several potentials. Flavor threshold has been estimated using eq. (16). (a) Inverse scattering, $\rho=1$, $m_b=4.5$ GeV/c^2; (b) inverse scattering, $\rho=1.4$, $m_b=4.75$ GeV/c^2; (c) inverse scattering, $\rho=2$, $m_b=5$ GeV/c^2 (all from ref. 3). (d) Richardson potential, ref. 10. (e) Buchmüller-Tye potential, with $\Lambda_{\overline{MS}}=0.2$ GeV; (f) Buchmüller-Tye potential, with $\Lambda_{\overline{MS}}=0.5$ GeV (both from ref. 10). The parameter $\Lambda_{\overline{MS}}$ is not well-determined, and may be varied between the values for which results are displayed.

Fig. 2: The ratio $R_{SP} \equiv [M(2S)-M(2P)]/[M(2S)-M(1S)]$ is plotted as a function of heavy-quark mass for the six potentials identified in the caption to Fig. 1. Also shown on the right-hand ordinate is the effective power which corresponds to particular values of R_{SP}.

Fig. 3: Leptonic widths of the 1S-4S levels of a heavy quarkonium family are displayed as functions of heavy-quark mass for the six potentials identified in the caption to Fig. 1. The heavy quark is assumed to be a color triplet, with electric charge $e_Q=2/3$.

Fig. 4: Relative positions of Υ and $(Q\bar{Q})$ levels in the $\rho=1.4$, $m_b=4.75$ GeV/c^2 potential. The $^3S_1$ levels are indicated by solid lines. The "even-parity" levels of the upsilon problem, which are explained in the text, are shown as dotted lines. Shaded bands denote the flavor threshold. (a) $m_Q=20$ GeV/c^2; (b) $m_Q=30$ GeV/c^2.

Fig. 5: Extrapolations in constituent mass for the reflectionless approximation to the logarithmic potential determined from the parameters in Table I. (a) The ratio of 2S-1S spacing to the true value. (b) The ratio of 2S-2P to 2S-1S intervals; the true value is shown by the dashed line. (c) The ratio of wavefunctions squared at the origin for the 2S and 1S levels; the true value is shown by the dashed line. (d) The ratio of extrapolated to true values of the square of the 1S wavefunction at the origin.

Fig. 6: Extrapolations in constituent mass for the reflectionless approximation to the Coulomb potential determined from the parameters in Table I. (a) The ratio of 2S-1S spacing to the true value. (b) The ratio of 2S-2P to 2S-1S intervals; the true value is shown by the dashed line. (c) The ratio of wavefunctions squared at the origin for the 2S and 1S levels; the true value is shown by the dashed line. (d) The ratio of extrapolated to true values of the square of the 1S wavefunction at the origin.

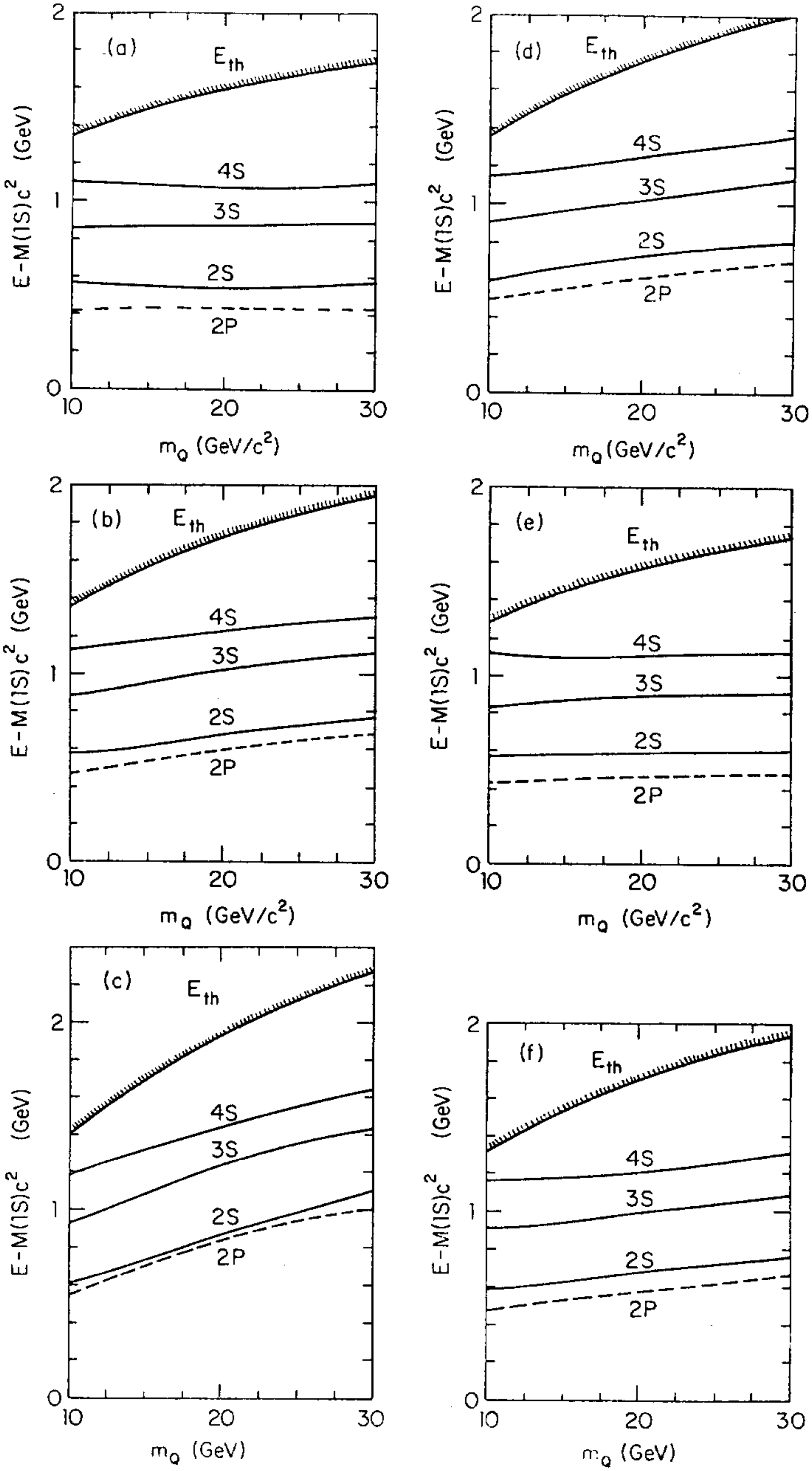

Fig. 1

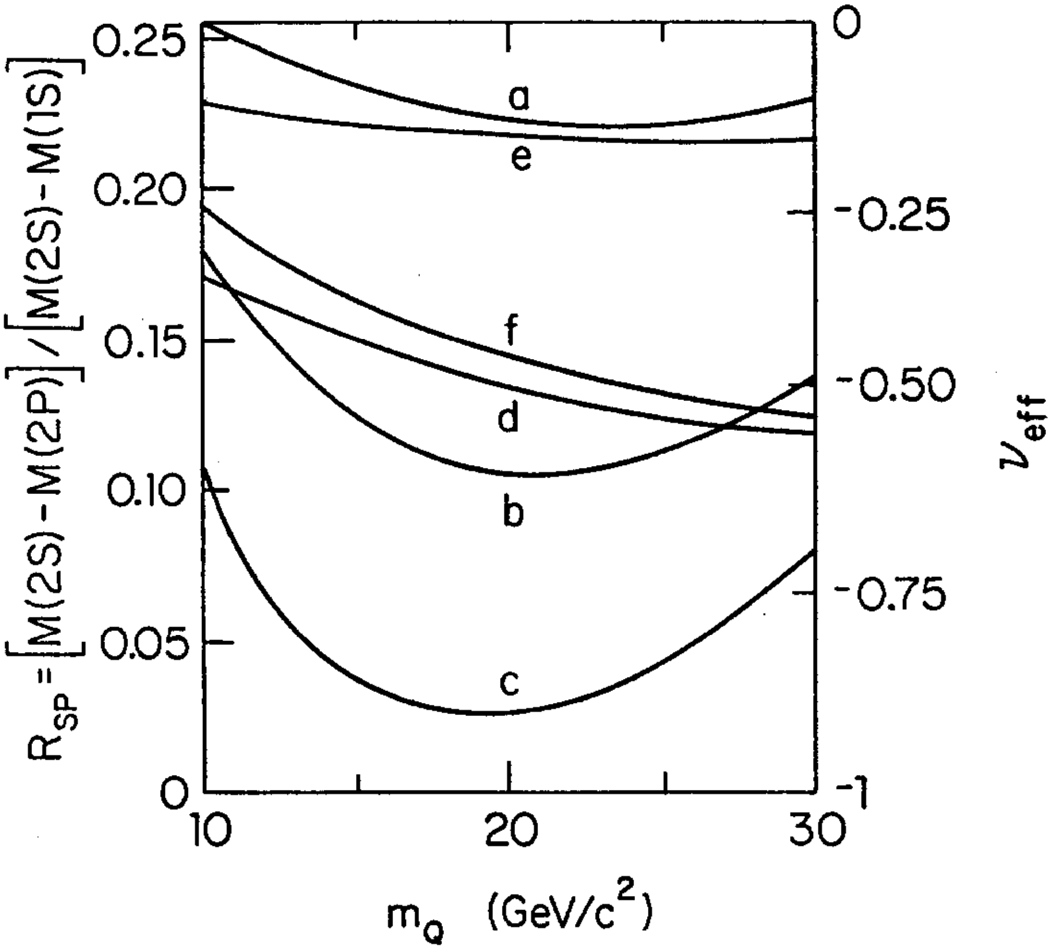

0.25
0.20
0.15
0.10
0.05
0
0
-0.25
-0.50
-0.75
-1
10
20
30
a
e
f
d
b
c
$R_{SP} = [M(2S) - M(2P)] / [M(2S) - M(1S)]$
ν_{eff}
m_Q (GeV/c^2)

Fig. 2

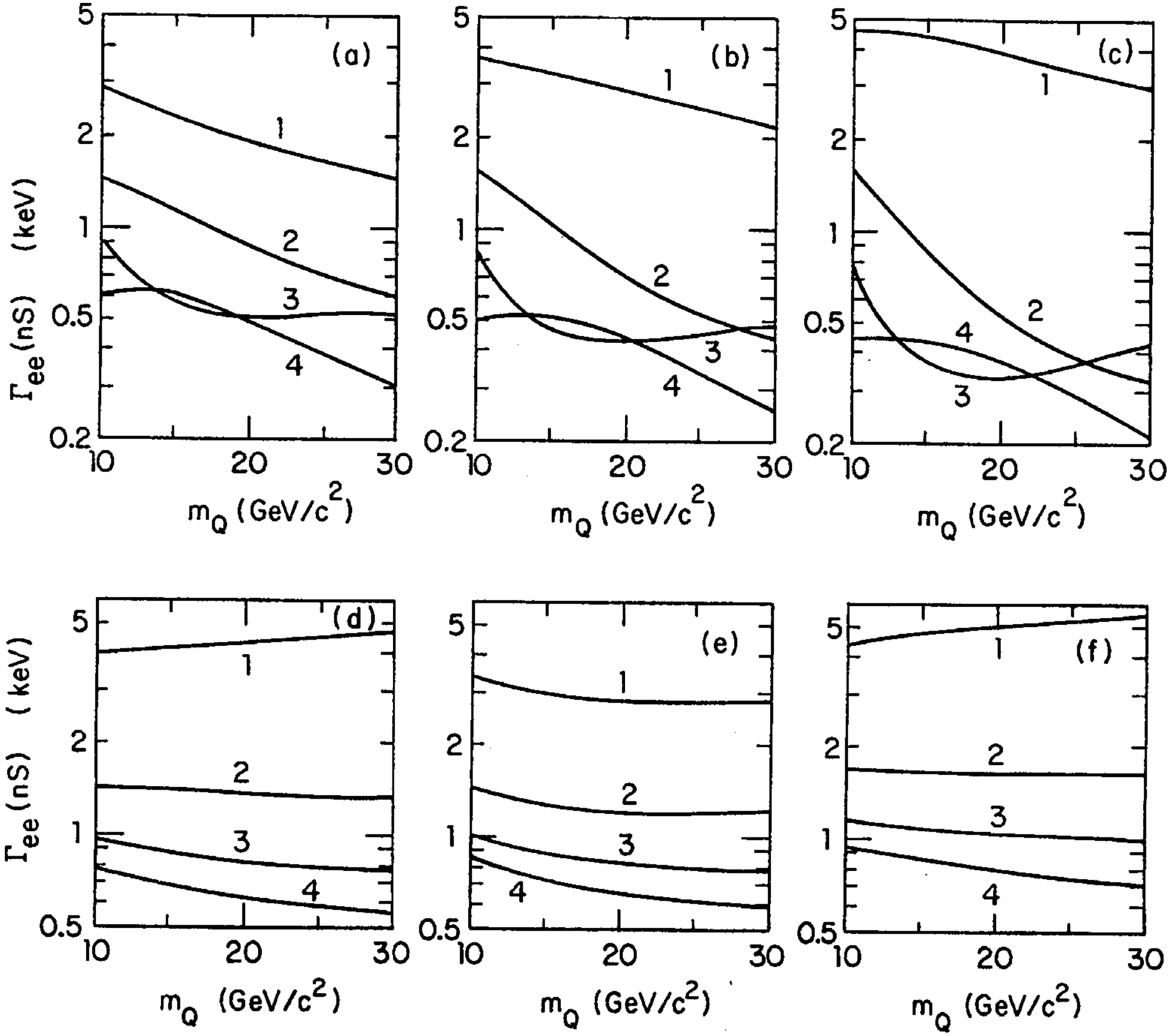

Fig. 3

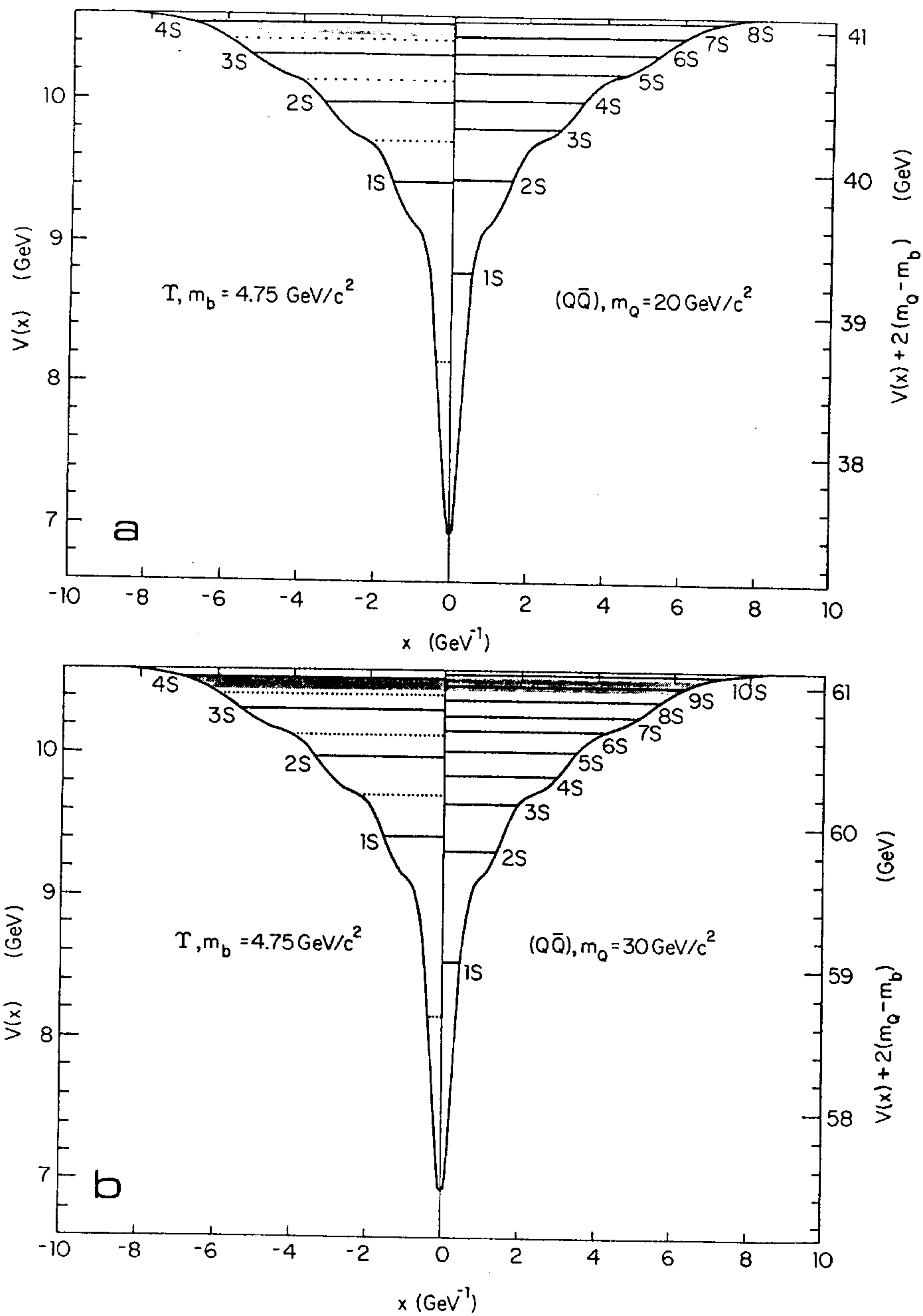

a
ϒ, m_b = 4.75 GeV/c²
(QQ̄), m_Q = 20 GeV/c²
V(x) (GeV)
V(x) + 2(m_Q − m_b) (GeV)
x (GeV⁻¹)
b
ϒ, m_b = 4.75 GeV/c²
(QQ̄), m_Q = 30 GeV/c²
V(x) (GeV)
V(x) + 2(m_Q − m_b) (GeV)
x (GeV⁻¹)

Fig. 4

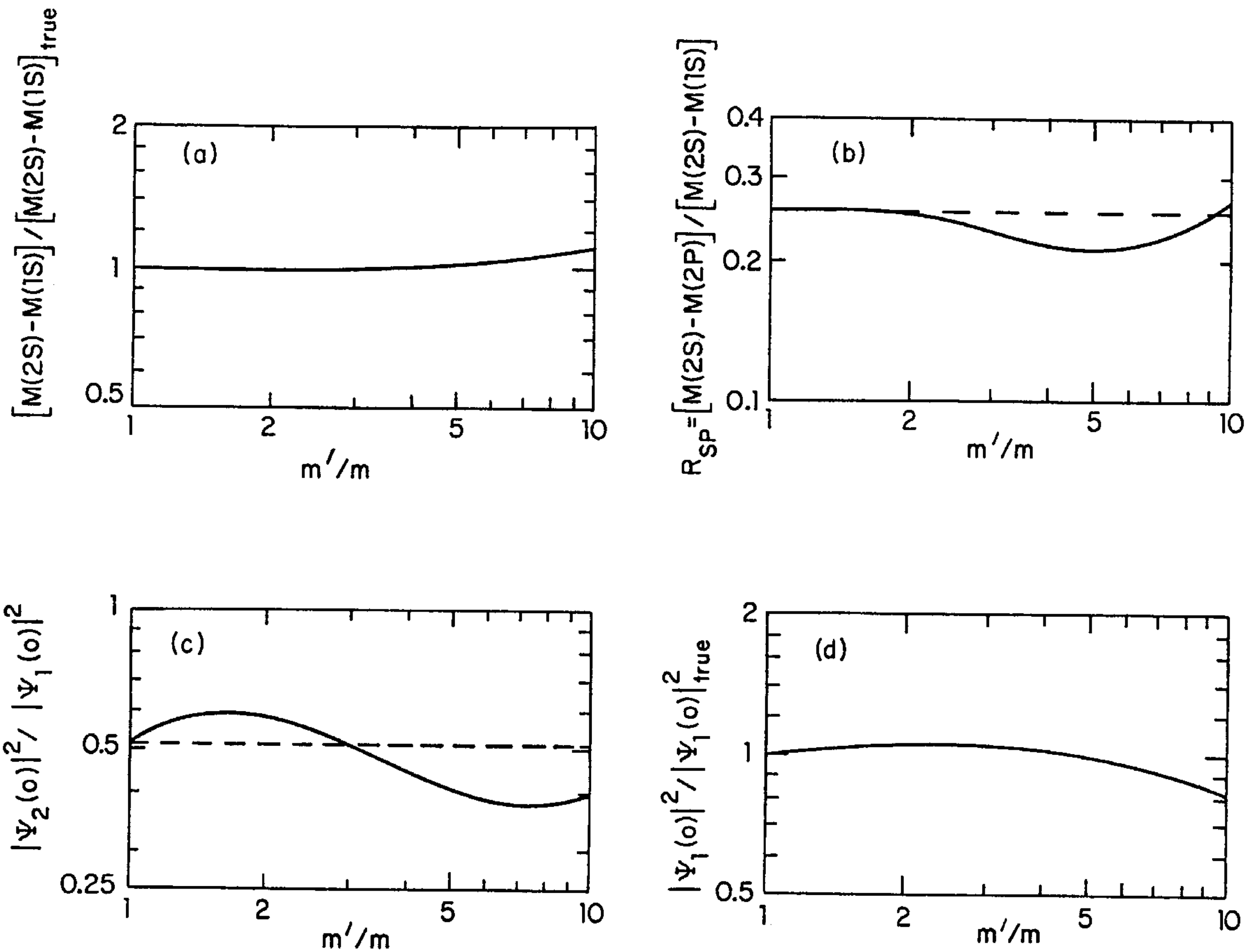
[M(2S)-M(1S)]/[M(2S)-M(1S)]true
2
1
0.5
(a)
1
2
5
10
m'/m
RSP=[M(2S)-M(2P)]/[M(2S)-M(1S)]
0.4
0.3
0.2
0.1
(b)
m'/m
|Ψ2(o)|2/ |Ψ1(o)|2
0.25
(c)
m'/m
|Ψ1(o)|2/|Ψ1(o)|2true
(d)
m'/m

Fig. 5

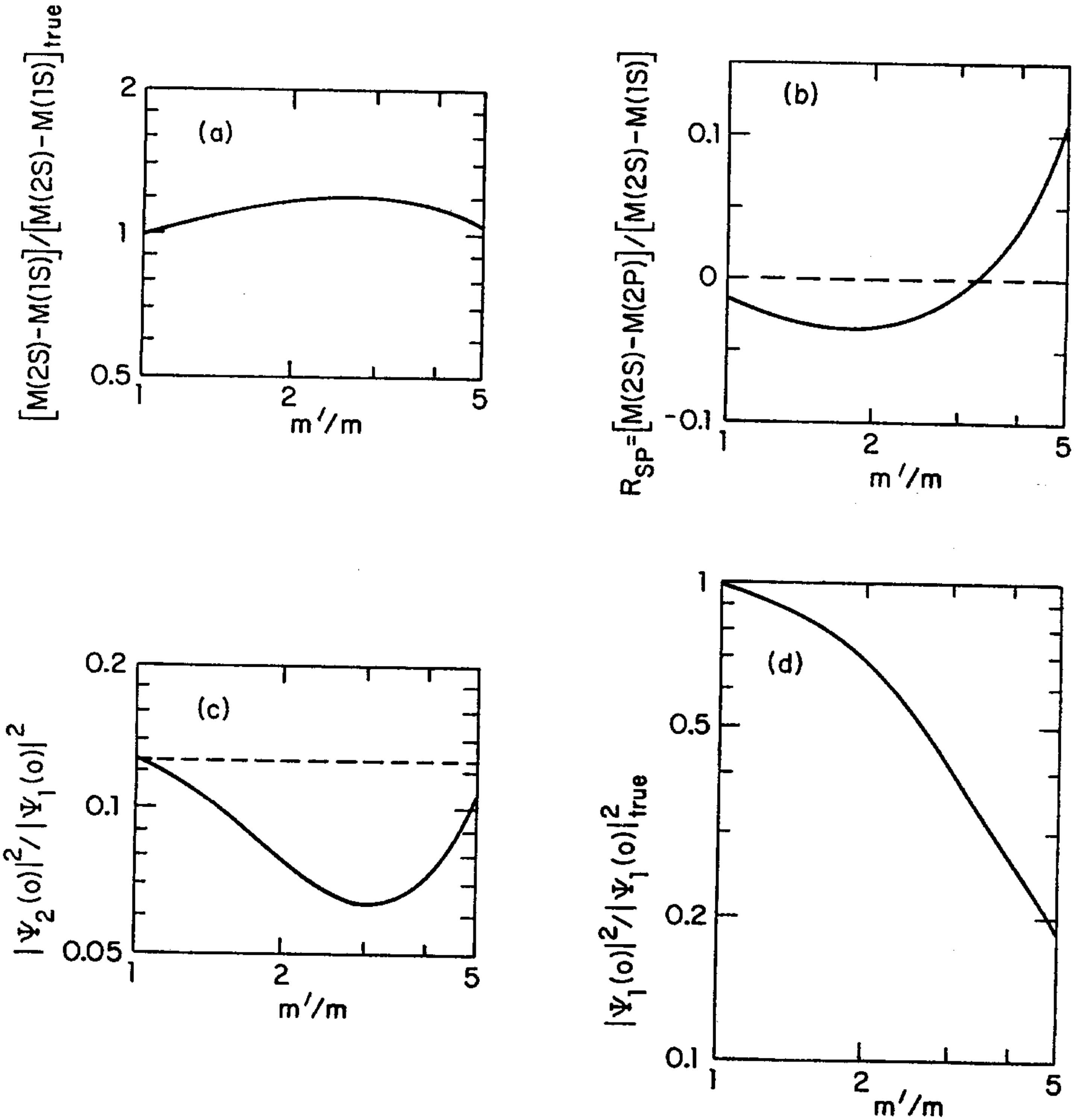

(a)
(b)
(c)
(d)
$[M(2S)-M(1S)]/[M(2S)-M(1S)]_{true}$
$R_{SP}=[M(2S)-M(2P)]/[M(2S)-M(1S)]$
$|\Psi_2(o)|^2/|\Psi_1(o)|^2$
$|\Psi_1(o)|^2/|\Psi_1(o)|^2_{true}$
m'/m
2
1
0.5
0.1
0
-0.1
0.2
0.05
5

Fig. 6